Ivana Jevtić[1], Jagoš Stojanović[2], Aleksa Milovanović[1], Isaak Trajković[1], Miloš Milošević[1], Goran Mladenović[2]

PRINTING ORIENTATION AND PLACE INFLUENCING THE COMPRESSIVE STRENGTH OF POLYAMID 12 SPECIMENS OBTAINED BY SLS TECHNOLOGY

UTICAJ ORIJENTACIJE I MESTA ŠTAMPE NA PRITISNU ČVRSTOĆU UZORAKA POLIAMIDA 12 DOBIJENIH SLS TEHNOLOGIJOM

Originalni naučni rad / Original scientific paper
UDK /UDC:

Rad primljen / Paper received: 1.11.2023

Adresa autora / Author's address
[1)] University of Belgrade, Innovation Centre of the Faculty of Mechanical Engineering, Belgrade, Serbia
email: ijevtic@mas.bg.ac.rs
[2)] University of Belgrade, Faculty of Mechanical Engineering, Belgrade, Serbia

Keywords
- SLS technology
- compressive testing
- Polyamide 12

Ključne reči
- SLS tehnologija
- ispitivanje na pritisak
- Poliamid 12

Abstract

This research aims to determine how the orientation and placement of printing impacts the compressive strength of specimens manufactured by Selective Laser Sintering (SLS). The research includes compressive specimens in which the CAD model dimensions are selected according to the ISO 604 standard, and specimen geometry Ø10×20 mm in bulk. All specimen configurations are additively manufactured in two different printing orientations, horizontal and vertical, and printed in the middle and on the edge of the powder bed. All specimens are additively manufactured using Polyamide 12 (PA 12) material on a Fuse 1 device (FormLabs, located in Summerville, MA). Compressive strength testing was carried out using a Shimadzu AGS-X universal testing machine (Shimadzu Corp., Kyoto, Japan).

Izvod

Istraživanje ima za cilj da se odredi kako orijentacija i položaj štampe utiču na pritisnu čvrstoću uzoraka proizvedenih korišćenjem tehnologije Selektivnog Laserskog Sinterovanja (SLS). Istraživanjem su obuhvaćeni uzorci na pritisak, kod kojih su dimenzije CAD modela odabrane prema standardu ISO 604, a izabrana geometrija uzorka je Ø10×20 mm. Svi uzorci su proizvedeni u dve različite orijentacije štampe, odnosno, horizontalnoj i vertikalnoj, i na dva mesta štampe, odnosno, štampane u sredini i na ivici sloja praha. Svi uzorci su aditivno proizvedeni korišćenjem materijala Poliamid 12 (PA 12) na uređaju Fuse 1 (FormLabs, iz Samervila, Masačusets, SAD). Za ispitivanje pritisne čvrstoće korišćena je univerzalna mašina za testiranje Shimadzu AGS-X (Shimadzu Corp. Kjoto, Japan).

INTRODUCTION

Additive Manufacturing (AM), often referred to as 3D printing, has witnessed an unprecedented evolution, revolutionizing the way we design and manufacture complex components across various industries, /1/. Among the multitude of AM techniques, selective laser sintering (SLS) stands out for its versatility and capability to produce intricate parts with high precision and efficiency. As SLS continues to find applications in fields such as aerospace, automotive, and medical devices, the quest for optimising material properties becomes ever more crucial.

Selective laser sintering (SLS) is an additive manufacturing technique that relies on powder bed fusion technology /2/. In this process, laser energy is precisely applied to selectively heat powder particles, causing them to partially melt and fuse together, ultimately solidifying them into a 3D structure using computer-aided design (CAD) /3, 4/. Figure 1 illustrates the structure and components of an SLS system. During the SLS process, it is crucial to maintain the temperature of the powder bed within a specific range known as the sinter window, which lies between crystallization and melting temperature, /5-7/. As a result, only semi-crystalline thermoplastics can be processed using SLS /5, 7/. The subsequent cooling phase is carefully controlled to prevent rapid recrystallization and promote the fusion of molten powder /6-8/. Rapid recrystallization can reduce dimensional accuracy, causing deformations and curling effects /6, 7/. Additionally, the outcome of the printing process is influenced by various parameters, including laser power, hatch distance, layer thickness, and scanning speed. Optimising these parameters while considering minimal distances between components enables efficient use of the building platform, allowing for the reuse of surrounding, non-solidified residual material /5, 7/. Besides the printing phase, the complete SLS process involves pre-processing and post-processing steps /5, 7, 9, 10/. Modern SLS 3D printers utilize different types of lasers, including diode, fibre, and carbon dioxide (CO_2) lasers, with CO_2 lasers being the most common. These lasers enable the creation of highly precise structures.

SLS is highly versatile and capable of producing a wide range of parts with different shapes, /12-13/. Among the materials suitable for SLS, polymers were among the first and are still widely used due to their low processing temperature, low laser power requirements, and high dimensional accuracy /14, 15/. Specifically, polyamide 12 (PA12) is the most frequently used semi-crystalline polymer in SLS applications across various industries, including medical, automotive, aerospace, and biomedical sectors, /16, 17/.

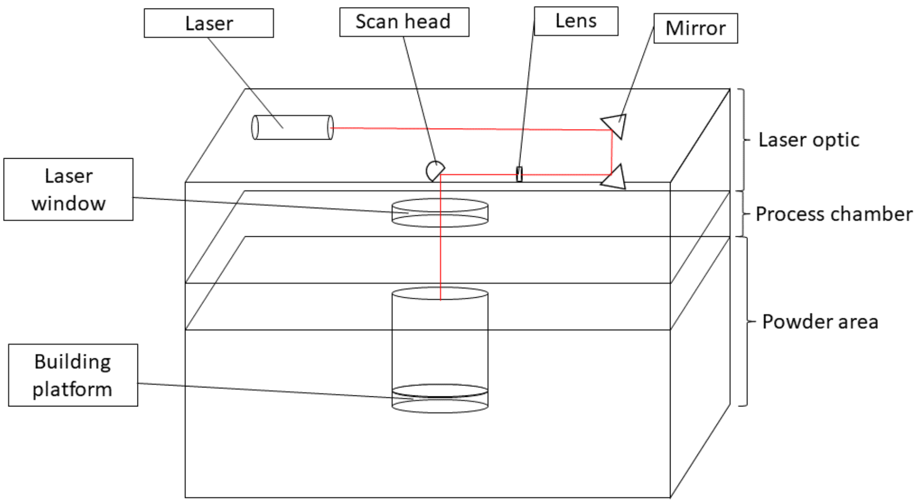

Figure 1. Design of an SLS system. Subdivision of the SLS system into three areas, /11/.

This paper presents an investigation into the mechanical properties of compression-printed polyamide 12 (PA12) specimens created using SLS technology. The study encompasses four series of specimens subjected to various compression orientations and locations within the powder layer. The primary objective of this research is to analyse the variations in compressive strength between horizontal and vertical compression orientations and between middle and edge printing locations within the powder layer. The findings from this study contribute to a deeper understanding of how different print orientations and powder bed locations affect the mechanical characteristics of materials produced with SLS technology.

MATERIALS AND METHODS

Materials

The study utilizes specimens generated from PA12 material (Formlabs, Sommerville, MA, USA) for research purposes. Polyamide 12 (PA 12) is a widely adopted material in the field of 3D printing, particularly in the realm of SLS technology. PA 12 showcases exceptional mechanical properties, including high tensile strength, robust impact resistance, and remarkable flexibility, making it highly suitable for the fabrication of functional and enduring components /18/. Notable mechanical characteristics of this material include a tensile strength of 50 MPa, flexural strength of 66 MPa, a modulus of elasticity of 1850 MPa, and compressive strength values of 13/24/55 MPa at 1, 2, 5 % strain, in respect, /19/.

CAD design

The cylindrical-shaped specimen having dimensions of 20 mm height and diameter of Ø10 mm, selected according to /20/ was designed using CAD software (SOLIDWORKS Premium® 2017 x64 Edition by Dassault systems). The CAD file is converted into .stl file, readable by printer software.

Method

Four specimen types are used for testing mechanical characteristics, i.e. compressive strength, according to standard /20/. Compressive specimens are Ø10×20 mm in bulk intended for compressive strength testing. All specimen configurations are additively manufactured in two different printing orientations, i.e., horizontal and vertical, and two printing locations, i.e., printing at the edge and on the middle of the powder bed. All specimens were produced on the Fuse 1 device (FormLabs, Summerville, MA), using polyamide 12 (PA 12) material. For purposes of the study, a total of four sets, each containing ten specimens, were produced, and the most promising specimens were selected for further investigation (see Fig. 2). Compressive specimens were produced separately, necessitating the completion of two distinct SLS processes.

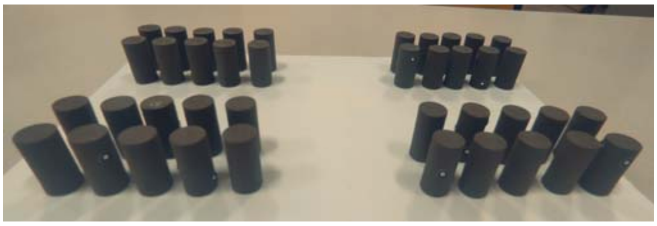

Figure 2. Four sets of compressive specimens.

Compressive specimens were printed in two directions: horizontal (HO_1-HO10 and HS_1-HS_10) and vertical (VO_1-VO_10 and VS_1-VS_10). HO stands for horizontally printed compressive specimens at the edge of powder bed, HS stands for horizontally printed compressive specimens in the middle of powder bed, VO stands for vertically printed compressive specimens at the edge of powder bed, VS stands for horizontally printed compressive specimens in the middle of the powder bed. All of the printed compressive specimens were tested on Shimadzu brand apparatus AGS-X of capacity 100 kN, and five of the best results we have taken into consideration (Fig. 3). The Shimadzu Autograph AGS-X series provides superior performance and practical testing solutions for a wide array of applications. Offering high-level control and intuitive operation, the AGS-X series sets a new standard for strength evaluations while providing the utmost in safety considerations in a modern design. Real-time auto-tuning of control parameters is offered, based on measured test force and strain data. Comparisons to unknown sample data are made safely without the need for preliminary tests. In addition, the 'autotuning function' easily performs strain control, as an ISO 6892-

2009 requirement. Specifications of the AGS-X 100 kN are /21/:

- capacity, 100 kN,
- dimensions, W945×D725×H2164 mm,
- test method files, 40 files (PC link: 20 files, standalone controller: 20 files),
- sampling speed, 1000 Hz max,
- effective test width, 600 mm,
- crosshead, table distance (tensile stroke), 1255 mm,
- crosshead speed accuracy, ±0.1 %,
- weight, 525 kg.

Figure 3. Testing on the Shimadzu AGS-100kNX.

To expand our research approach, we can incorporate optical systems, such as 3D scanners and digital image collection (DIC) techniques. In the context of additive manufacturing, 3D scanners are frequently employed for dimensional analysis of polymer and composite materials, while DIC is utilised to assess deformations in structures subjected to various types of loading, /22-25/.

RESULTS AND DISCUSSION

Tables 1-4 show testing results. Charts 1-4 are made for each test. In Table 1, elongation test results for specimens printed horizontally are presented at 1, 2, and 5 % deformation, with compressive strengths 13, 24, and 55 MPa, in respect. Notably, the 5 % deformation level exhibits the least deviation from the expected PA12 material properties.

Table 1. Results of HO series testing.

	Compressive strength 1 %	Compressive strength 2 %	Compressive strength 5 %
HO_1	5.60	18.51	53.96
HO_2	6.10	18.58	52.14
HO_3	5.55	17.58	50.74
HO_4	5.69	17.85	50.99
HO_5	4.15	16.81	54.06
Average_HO	5.42	17.87	52.38

Table 2 shows elongation results of 1, 2, and 5 % of horizontally printed specimens in the middle of the powder bed. As with the HO and HS test specimens, the smallest deviation obtained by testing in relation to the value of the PA 12 material is at 5 % deformation.

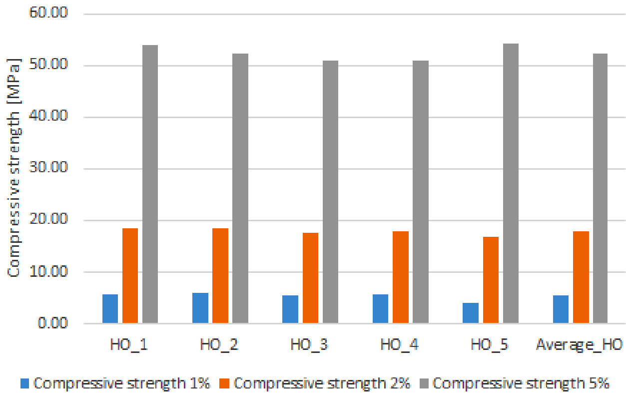

Chart 1. Testing of HO Series.

Table 2. Results of HS series testing.

	Compressive strength 1 %	Compressive strength 2 %	Compressive strength 5 %
HS_1	6.17	19.18	54.27
HS_2	5.10	17.91	55.44
HS_3	4.39	13.79	48.53
HS_4	5.66	16.87	53.72
HS_5	4.58	14.32	53.97
Average_HS	5.18	16.41	53.19

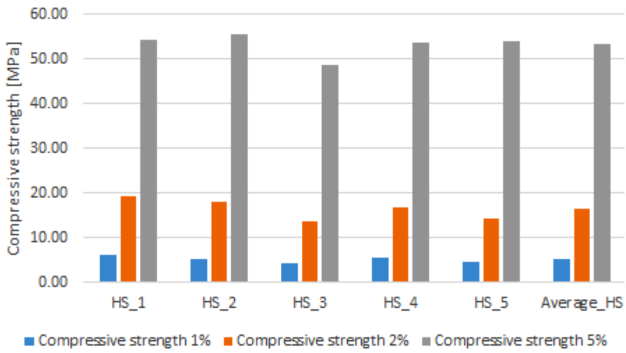

Chart 2. Testing of HS Series.

The compressive strength of vertically printed specimens on the perimeter of the powder bed is shown in Table 3. Based on the obtained results, it can be observed that the compressive strength values at 1 and 2 % deformation are quite different from PA 12 compressive strength.

Table 3. Results of VO series testing.

	Compressive strength 1%	Compressive strength 2%	Compressive strength 5%
VO_1	5.64	18.68	51.82
VO_2	6.04	18.64	49.72
VO_3	6.25	19.89	52.69
VO_4	5.17	18.14	51.74
VO_5	5.24	18.25	51.63
Average_VO	5.67	18.72	51.52

Table 4 shows the compressive strength of specimens that were vertically printed in the middle of the powder bed. Notably, the compressive strength values at 1 and 2 % deformation markedly differ from those associated with the PA 12. The lowest average compressive strength during the elongation of 2 % is for compressive specimens printed in the VS series direction.

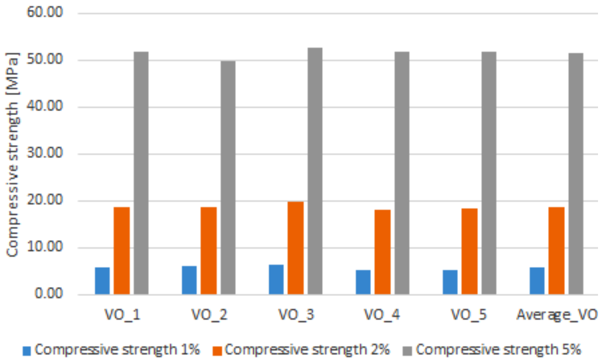

Chart 3. Testing of VO Series.

Compressive strength averages at 1, 2, and 5 % deformation are illustrated on the graph. It is worth noting that HS samples exhibit the highest compressive strength at 5 % deformation, and this value closely aligns with the inherent strength of the PA 12 material.

Table 4. Results of VS series testing.

	Compressive strength 1 %	Compressive strength 2 %	Compressive strength 5 %
VS_1	4.90	16.31	51.96
VS _2	4.96	16.69	52.29
VS _3	4.62	16.53	52.20
VS _4	4.62	15.54	51.47
VS _5	4.63	15.51	51.76
Average_VS	4.75	16.12	51.94

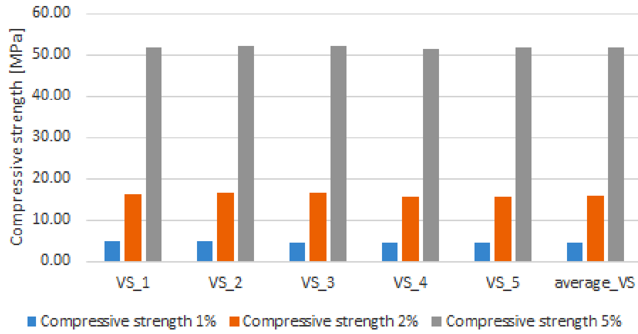

Chart 4. Testing of VS Series.

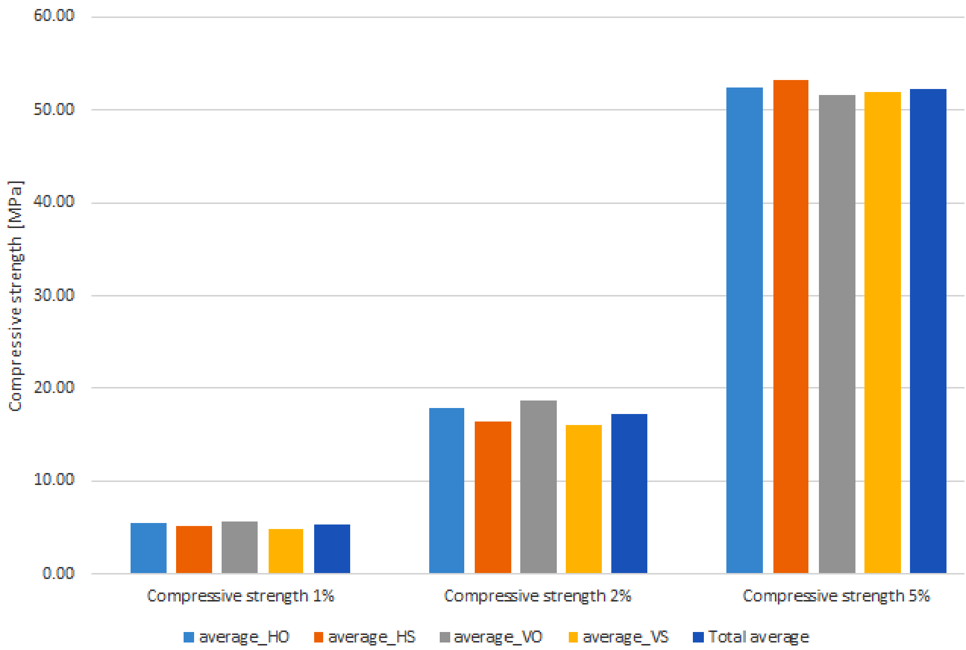

Chart 5. Comparative analysis of all testing.

CONCLUSIONS

This research paper presents a comprehensive analysis of compressive specimens that were crafted through the innovative technique of selective laser sintering, using polyamide PA12 as the primary material. The primary objective of this study was to delve deep into the mechanical properties of these additively manufactured specimens, scrutinizing them from various perspectives, including print orientation and location.

Our results indicate that the mechanical characteristics of the printed components show minimal variations regardless of print orientation and placement. This discovery contradicts the traditional belief that these variables could have a substantial influence on the mechanical properties of additively manufactured parts.

However, what stands out as particularly noteworthy from our research is the substantial difference in compressive strength values at 1 and 2 % deformation when compared to the base PA12 material. In fact, the compressive strength at 1 % deformation is observed to be a staggering 60 % lower than that of PA12 material. This revelation opens up possibilities for further research and analysis, prompting questions about the underlying reasons for this significant divergence in mechanical properties.

In summary, this study represents a valuable addition to the realm of additive manufacturing. It offers a deeper understanding of intricate responses of selectively laser sintered polyamide PA12 specimens when subjected to compressive loads. These discoveries not only challenge established beliefs about the effects of print orientation and placement but also beckon for more comprehensive investigations into the distinct properties of these additively produced components. These insights hold the promise of driving improvements in the optimisation of 3D printing processes and materials, with potential ramifications for diverse sectors, including aerospace and healthcare.

ACKNOWLEDGEMENTS

The authors acknowledge the support from the Ministry of Education, Science and Technological Development of the Republic of Serbia, contracts: 451-03-47/2023-01/200213.

REFERENCES

1. Li, K., Yang, T., Gong, N., et al. (2023), *Additive manufacturing of ultra-high strength steels: A review*, J Alloys Compd. 965: 171390. doi: 10.1016/j.jallcom.2023.171390
2. ASTM F2792-12a: Standard Terminology for Additive Manufacturing Technologies, ISO, Geneva, Switzerland, 2013. doi: 10.1520/f2792-12a
3. Charoo, N.A., Barakh Ali, S.F., Mohamed, E.M., et al. (2020), *Selective laser sintering 3D printing - an overview of the technology and pharmaceutical applications*, Drug Dev. Ind. Pharm. 46(6): 869-877. doi: 10.1080/03639045.2020.1764027
4. Awad, A., Fina, F., Goyanes, A., et al. (2021), *Advances in powder bed fusion 3D printing in drug delivery and healthcare*, Adv. Drug Deliv. Rev. 174: 406-424. doi: 10.1016/j.addr.2021.04.025
5. Gibson, I., Rosen, D., Stucker, B., Additive Manufacturing Technologies: 3D Printing, Rapid Prototyping and Direct Digital Manufacturing, 2nd Ed.; Springer: New York, NY, 2015. ISBN 978-1-4939-2112-6
6. Goodridge, R.D., Tuck, C.J., Hague, R.J.M. (2012), *Laser sintering of polyamides and other polymers*, Prog. Mater. Sci. 57 (2): 229-267. doi: 10.1016/j.pmatsci.2011.04.001
7. Schmid, M., Selektives Lasersintern (SLS) mit Kunststoffen: Technologie, Prozesse und Werkstoffe, Hanser: München, Germany, 2015. ISBN 978-3-446-44562-8
8. Dadbakhsh, S., Verbelen, L., Verkinderen, O., et al. (2017), *Effect of PA12 powder reuse on coalescence behaviour and microstructure of SLS parts*, Europ. Polym. J, 92: 250-262. doi: 10.1016/j.eurpolymj.2017.05.014
9. Celik, E., Additive Manufacturing, Science and Technology, De Gruyter: Berlin, Germany, 2020. doi: 10.1515/9781501518782
10. Seppala, J.E., Kotula, A.P., Snyder, C.R. (Eds.), Polymer-Based Additive Manufacturing: Recent Developments, American Chemical Society, Washington DC, USA, 2019. doi: 10.1021/bk-2019-1315
11. Eggers, T., von Lacroix, F. (2023), *Investigation of the influence of the mixing process on the powder and component properties during cyclic reuse of a polyamide 12 sinter material in selective laser sintering*, Powders, 2(1): 75-96. doi: 10.3390/powders2010006
12. Fina, F., Goyanes, A., Madla, C.M., et al. (2018), *3D printing of drug-loaded gyroid lattices using selective laser sintering*, Int. J Pharmac. 547(1-2): 44-52. doi: 10.1016/j.ijpharm.2018.05.044
13. Awad, A., Fina, F., Trenfield, S.J., et al. (2019), *3D printed pellets (miniprintlets): a novel, multi-drug, controlled release platform technology*, Pharmac. 11(4): 148. doi: 10.3390/pharmaceutics11040148
14. Awad, A., Fina, F., Goyanes, A., et al. (2020), *3D printing: Principles and pharmaceutical applications of selective laser sintering*, Int. J Pharm. 586: 119594. doi: 10.1016/j.ijpharm.2020.119594
15. Yan, C., Shi, Y., Hao, L. (2011), *Investigation into the differences in the selective laser sintering between amorphous and semi-crystalline polymers*, Int. Polym. Process. 26(4): 416-423. doi: 10.3139/217.2452
16. Feng, L., Wang, Y., Wei, Q. (2019), *PA12 powder recycled from SLS for FDM*, Polymers, 11(4): 727. doi: 10.3390/polym11040727
17. Paolucci, F., van Mook, M.J.H., Govaert, L.E., Peters, G.W.M. (2019), *Influence of post-condensation on the crystallization kinetics of PA12: From virgin to reused powder*, Polymer, 175: 161-170. doi: 10.1016/j.polymer.2019.05.009
18. Martynková, G.S., Slíva, A., Kratošová, G., et al. (2021), *Polyamide 12 materials study of morpho-structural changes during laser sintering of 3D printing*, Polymers, 13(5): 810. doi: 10.3390/polym13050810
19. Formlabs: https://formlabs-media.formlabs.com/datasheets/2001447-TDS-ENUS-0.pdf (accessed on 17 January 2024).
20. ISO 604: Plastics - Determination of compressive properties, ISO, Geneva, Switzerland, 2002.
21. Shimadzu: https://www.ssi.shimadzu.com/products/materials-testing/uni-ttm/autograph-ags-x-series/spec.html (accessed on 17 January 2024).
22. Jevtić, I., Mladenović, G., Milošević, M., et al. (2022), *Dimensional accuracy of parts obtained by SLS technology*, Struct. Integr. Life, 22(3): 288-292.
23. Nikitović, A., Pešić, D., Kolak, V., et al. (2023), *3D digital image correlation analysis of local deformation field of different endodontic calcium silicate cements*, Appl. Sci. 13(3): 1633. doi: 10.3390/app13031633
24. Mitrović, N., Milošević, M., Sedmak, A., et al. (2011), *Application and mode of operation of non-contact stereometric measuring system of biomaterials*, FME Trans. 39(2): 55-60.
25. Milošević, M., Mitrović, N., Jovičić, R., et al. (2012), *Measurement of local tensile properties of welded joint using Digital Image Correlation method*, Chemicke Listy, 106: 485-488.